GSA DATA REPOSITORY 2019119

Blackburn, T., et al., 2019, Composition and formation age of amorphous silica coating glacially polished surfaces: Geology, https://doi.org/10.1130/G45737.1

Appendix DR1. Sample locations and additional compositional data. The Glacial polish samples studied here were collected from Yosemite National Park (YNP), California. A total of 6 samples from the Lyell canyon and Tuolumne meadows area, were used to collect major and trace element data (Fig. DR1.1). Lyell and MaClure samples were collected from elevation, towards the glacier accumulation area for this catchment, while DAFF is located farther below (Fig. DR1.1).

In figure 2 of the main text the major and trace element data for DAFF dome is presented. For brevity, this figure excluded Al_20_3 and Th. These additional elements for DAFF dome are presented here as a modified version of the figure 2 included in the main text (Fig. DR1.2). The same compositional analysis was performed on the 5 additional MaClure and Lyell basin samples. These data are presented within this appendix as figures DR1.3-1.7. A k-means cluster analysis from MATLAB was performed on these data to identify the polish composition and underlying minerals for each spot analysis. A k-means cluster analysis partitions the calculated element concentrations at each ablation depth into one of two clusters (defined by user) with the nearest mean. The center of each cluster is a collection of values that are interpreted to best define the resulting group. These data (black circles) are what is presented in the main text's figure 3.

Appendix DR2. LA-ICPMS methods and Data Reduction

All LA-ICPMS analyses were conducted using a Photon Machines Analyte 193H Excimer Laser outfitted with Helex 2-Volume Cell feed into a Thermo Scientific X-series quadrupole ICP-MS. Laser spot sizes were set to 25 μm, a minimum size found to meet instrument detection limits for selected major elements: Na, Mg, Al, Si, Ca, Fe. Elements U and Th were also measured but often below detection limits, in particular at depth within host minerals. Laser parameters include: 80 bursts at a 4Hz shot rate. Sample unknowns were measured along with standard NIST-610. Spot analyses were conducted by ablating from the glacially polished surfaced downwards through the amorphous layer and into the coarse minerals of the underlying host rock. It was not possible to utilize the traditional LA-ICPMS data reduction technique of internal normalization because the proportions of all elements change within this depth profile. We instead adopted a sum-normalization technique, applied to each cycle of masses within the ICPMS data. By dividing the proportions of each cycle by the sum we can roughly determine the relative proportions of each element as a function of depth. This data reduction includes: 1) blank correction; 2) conversion of signal intensities (cps) to elemental concentrations using measured NIST 610 intensities; 3) Conversion of isotopic concentrations to total elemental abundances; 4) Conversion of elemental concentrations to oxides; 5) Normalization of the total oxide for a given mass cycle. We find that the sum normalization technique leaves this final data output from this reduction technique highly insensitive to data reduction steps 2 and 3. Rather the results seemingly deliver a reliable measure of the relative proportion of elements at any depth for a given analyses. It thus remains only to evaluate whether there is inherit bias with a single spot analyses between shallow and deep parts of the laser pit, which we will address below. Our use of this "sum-normalization" techniques makes several assumptions including: 1) That sum normalization is not "missing" any large component of the material (e.g. that Na, Mg, Al, Si, Ca, Fe, U and Th constitute 99% or more of the total material). 2) That element allocation in oxides is valid 3) that elemental fractionation in the NIST standards is identical to the samples, and 4) that down hole changes do occur but they do not cause elemental fractionation (e.g. the relative delivery of different to the mass spectrometer remains constant during spot analyses.

We can evaluate all of these assumptions by through collection and reduction of secondary standard data. Here we present LA-ICPMS analyses from ATHO (Fig. DR1.1) and a analyses collected from multiple minerals on a manually polished section of Cathedral Peak Granodiorite (Fig. DR2.2). The ATHO analyses reveal that there is no inherent bias corresponding with sample depth (e.g. blue and yellow data points cluster in same region). This implies that the compositional trends comparing shallow amorphous material and the underlying host minerals remains a viable conclusion for this paper. This statement is supported by the data collected from a manually polished sample of Cathedral peak granodiorite. The compositional of host minerals are discrete resolved with compositions independent of ablation depth (Fig. DR2.2). These secondary data no not nearly as precise (~10% uncertainties) as other in situ techniques (i.e. electron microprobe), however the technique provides the ability to measure continuous compositional not offered by other these more precise methods.

Appendix DR3: SHRIMP ^{230}Th, ^{232}Th, ^{234}U, ^{238}U analytical methods and data reduction

Opal in situ U-Th isotopic measurements were performed using the SHRIMP-RG (sensitive high-resolution ion microprobe with reverse geometry) operated by Stanford University and the U.S. Geological Survey during five analytical sessions between March 2017 and July 2018. Fragments (10 to 24 mm) Daff granite with polish coating was cast in a 25 mm diameter epoxy disc with pre-polished reference materials (BZVV opal and NIST-SRM-611 glass. BZVV is a ca. 2.83 Ma porcelaneous biogenic opal (Virgin Valley, NV, USA), that is relatively high U (748-888 ppm U) used as a secular equilibrium reference material (Paces et al., 2004; Amelin and Back, 2006). The mounted samples were rinsed with a 10% EDTA solution (ethylenediaminetetraacetic acid) and thoroughly rinsed in distilled water and dried in a vacuum oven. The sample surface was coated with ~100 nm Au and inspected to ensure uniformity and conductivity, stored in a pre-evacuation chamber at ~10-7 torr overnight prior to analysis to minimize degassing of the epoxy.

All analyses were performed by depth profiling through the surface into the amorphous silica polish. Because the polish is relatively thin and low U, the objective was to obtain a large spot (30-50 microns) that was as flat-bottomed as possible to minimize the sputter rate while maximizing secondary ion intensity. The second analytical session utilized an O- primary ion beam with intensity ranging from 45-55 nA. Although the secondary ion yield was ~35% higher using O-, the sputter rate was higher and thus sputtered through the polish more quickly. Therefore, for all subsequent sessions, we used an O2- primary ion beam with intensity ranging from 12-19 nA. The acquisition routine included the following masses: 28Si416O5+, 197Au+, 238U+,232Th12C+, 232Th16O+, background measured at 0.05 m/z above 232Th16O, 234U16O+ and 238U16O+. All peaks were measured on a single ETP® discrete-dynode electron multiplier operated in pulse counting mode. Analyses were performed with 9-12 scans (peak-hopping cycles from mass 192 through 254) and count times for 232Th16O and 234U16O+ ranging from 90 to 120 seconds and 35 to 50 seconds, respectively. Individual analyses took 45 to 60 minutes and with sputtered pit depths estimated to be 5-8 μm. Measurements were performed at mass resolutions of $M/\Delta M$ = 7,000-8,500 (10% peak height) to avoid interfering isobaric interferences.

Measured isotopic ratios were corrected for detector deadtime, background, and calculated cycle-by-cycle (i.e., depth into the polish). As discussed in the text, not all the polish material is amorphous silica or enriched in U; the surface layer (typically <1 μm thick; Fig. 1) can be phyllosilicate alteration and polish can contain micron- to submicron-sized mineral fragments in secular equilibrium. As a result, the initial scan intersecting phyllosilicate material was typically omitted. Additionally, scans lacking U and 230Th or those in secular equilibrium were also omitted, which typically were deeper in the sputter pits (scan number >8), likely due to intersection of mineral fragments or the underlying host minerals that lack U and/or were in secular equilibrium. Based on these criteria, typically 30-80% of the measurement results were used from each spot, and ratios were calculated using methods outlined by Ludwig (2009) with calculated into activity ratios (AR) using 238U, 232Th, 230Th, and 234U decay constants of 1.55125×10-7, 4.9475×10-8, 0.0091577, 0.002834, respectively. BZVV opal reference material were repeatedly measured throughout the analytical sessions.

Measured 238U/232Th AR and 230Th/238U AR were corrected for correct for mass discrimination based on session-averaged measurements of 230Th/238U for BZVV, which should be unity based on U-Th isotopes measurements Amelin and Back (2006) and measurements of a similar opal, M-21277, from the same locality by Paces et al. (2004). Uranium concentrations for glacial polish were calculated relative to BZVV opal, using an average concentration of 840 ppm U from Amelin and Back (2006).

This geochronologic method used in figure 4 assumes that upon formation, this fractionation was complete (e.g. 230Th/238U ~0), an assumption that is supported by a regressed 230Th/232Th activity ratio initial for the Daff Dome polish of 1.6±1.3 (Fig. DR. 3.1).

References

Amelin, Y., and Back, M., 2006, Opal as a U–Pb geochronometer: Search for a standard: Chemical Geology, v. 232, p. 67-86.

Ludwig, K. R., 2009, SQUID 2: A User's Manual, rev. 12. Berkeley Geochron. Ctr. Spec. Pub. 5 110 p.

Paces, J.B., Neymark, L.A., Wooden, J.L. & Persing, H.M., 2004, Improved spatial resolution for U-series dating of opal at Yucca Mountain, Nevada, USA, using ion-microprobe and microdigestion methods, Geochimica et Cosmochimica Acta, v. 68, p. 1591-1606.

Appendix DR4. Ablation rate determination: We can empirically calibrate the depth at which compositional changes occur by ablating samples for a range of laser pulses from 5 to 80 and with inferometer measurements of laser pit depths (Fig. DR 4.1) These data are used to assign approximate depths to compositional data (Fig. 1-2). A total of 80 pulses were used for all analyses presented in this manuscript. The ablation rate varies between 0.08 μm/pulse at shallow depths decreasing to 0.05-0.06 μm/pulse at greater depths (Fig. DR4.1). A maximum 0.08 μm/pulse was assumed to the depth assignments in figures 1 and 2 of the main text. This rate does not influence the data reduction in any way and only permits rough estimates on the depth of chemical transitions to be assigned.

Table. DR1.1 Sample locations.

Sample name	**Coordinate**	**N**	**W**
Daff	37°52'39.4"N 119°24'52.3"W	37.877611	-119.414528
Lyell08	37°45'17.5"N 119°15'35.6"W	37.754861	-119.259889
Lyell09	37°45'20.3"N 119°15'35.3"W	37.755639	-119.259806
Lyell10	37°45'24.2"N 119°15'57.5"W	37.756722	-119.265972
Maclure03	37°45'16.1"N 119°16'52.6"W	37.754472	-119.281278
Maclure05	37°45'56.2"N 119°16'25.8"W	37.765611	-119.273833

Fig. DR1.1

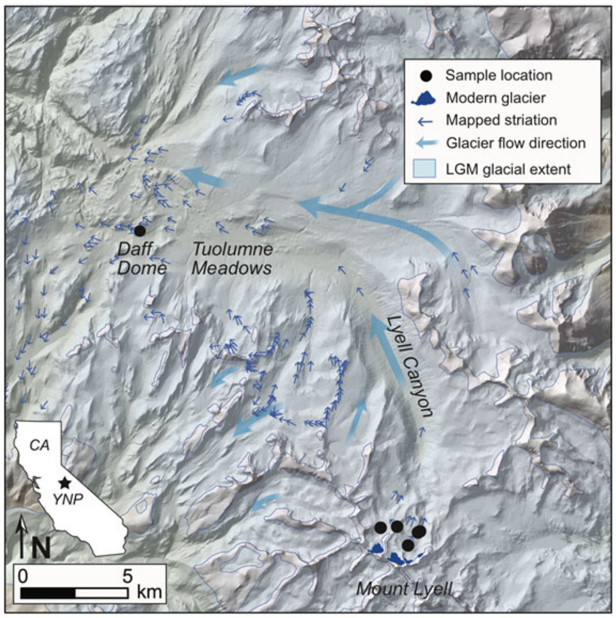

Figure DR1.1 Map of Lyell Canyon and Tuolumne Meadows, Yosemite National Park (YNP), CA. Compositional data were collected on 6 samples near the top of the Lyell canyon catchment, and 1 at Daff dome. U-series analyses were only conducted on the sample collected from Daff dome.

Figure DR 1.2.

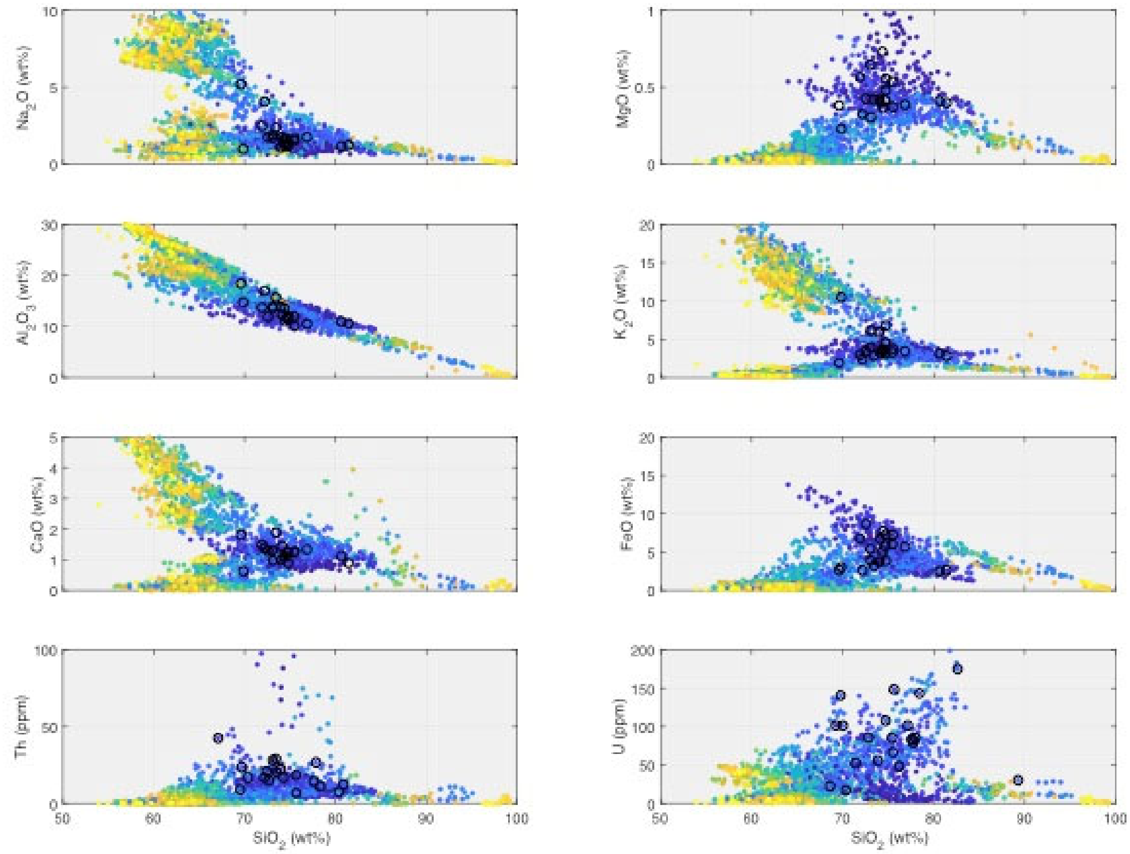

Figure DR1.2 Compositional data from Daff dome. The same data presented in Figure 2 of the main text, presented here with Al_2O_3 and Th data.

Figure DR 1.3

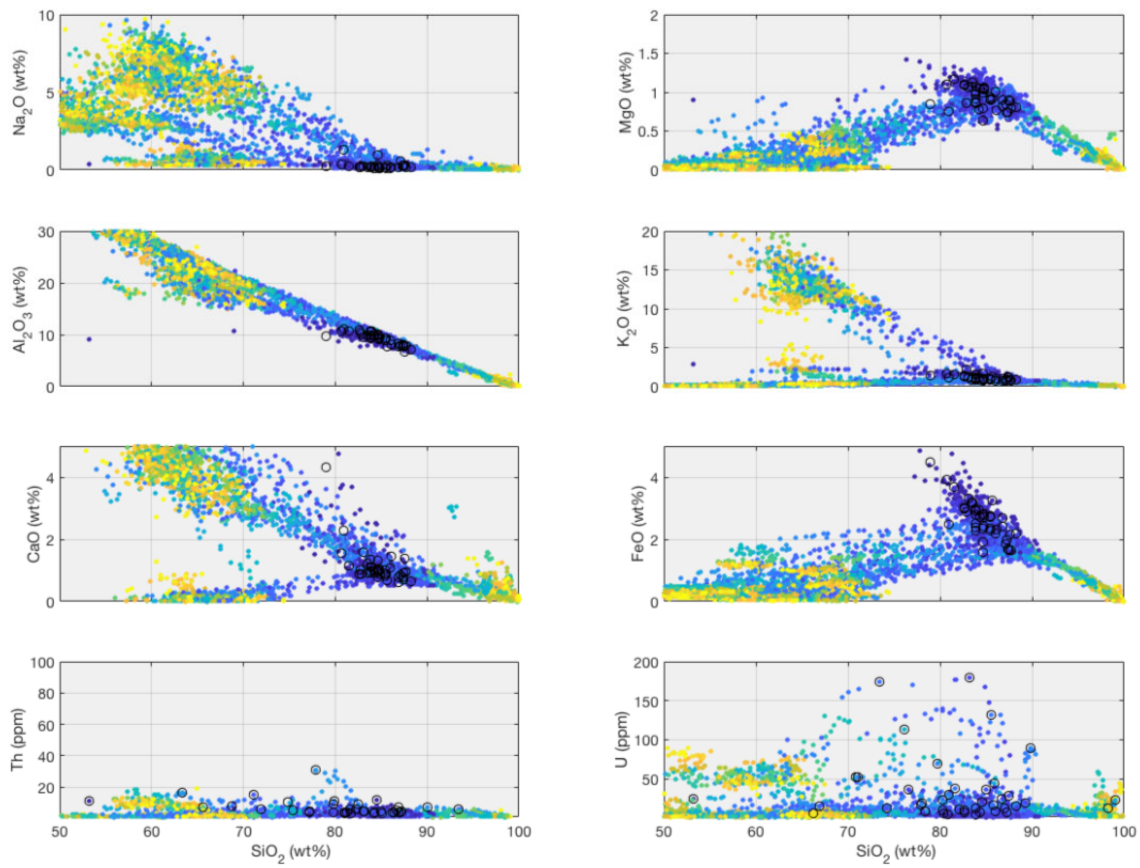

Figure DR1.3 Compositional data from sample MaClure03. Polish compositions for each laser spot analysis are defined as black circles and presented in Figure 3 of the main text. As in figure 2, yellow colors are deep reflecting the bottom of laser pits and the composition of underlying host minerals, while blue colors mark shallow depths and that of the glacial polish. Ablation rate was not calibrated for this sample, thus depths are relative.

Figure DR 1.4

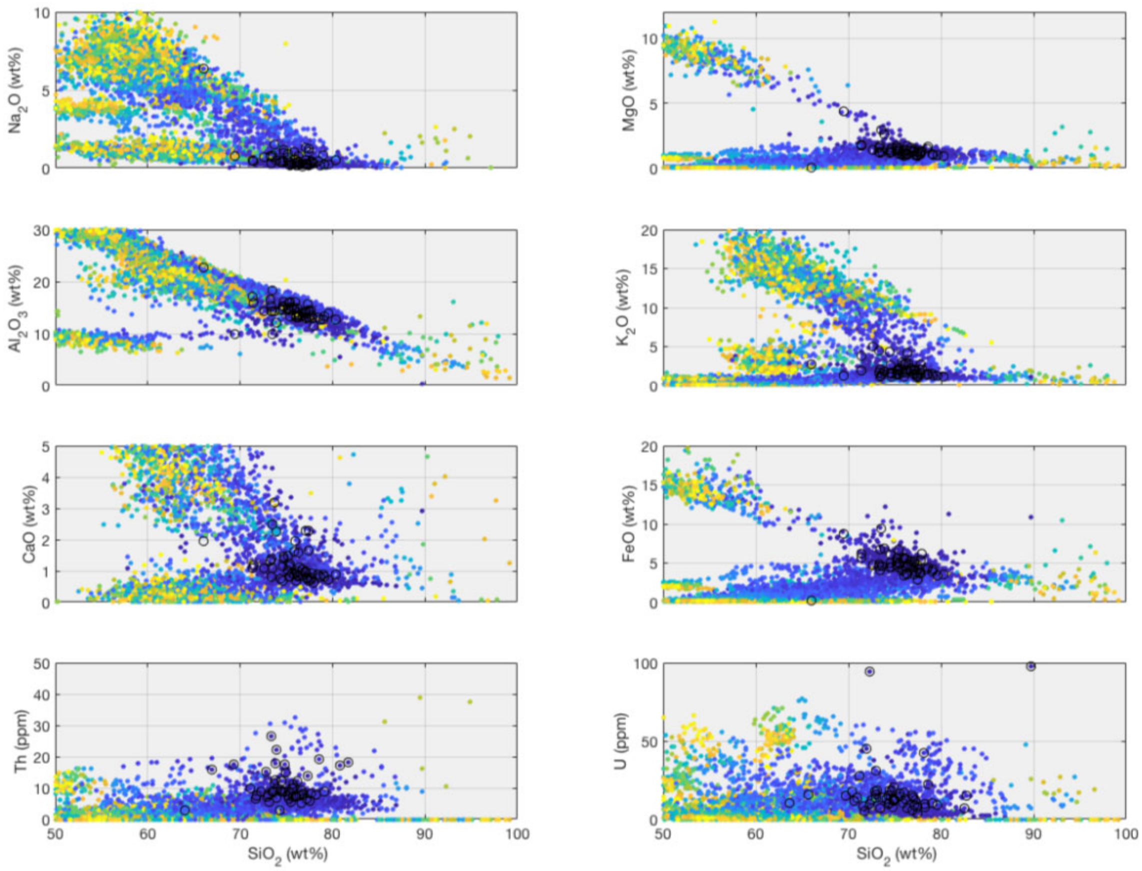

Figure DR1.4 Compositional data from sample MaClure05. Polish compositions for each laser spot analysis are defined as black circles and presented in Figure 3 of the main text. The polish covering high Fe and Mg amphiboles are was measured on this sample, with compositions the same as those above quartz and feldspar. As in figure 2, yellow colors are deep reflecting the bottom of laser pits and the composition of underlying host minerals, while blue colors mark shallow depths and that of the glacial polish. Ablation rate was not calibrated for this sample, thus depths are relative.

Figure DR 1.5

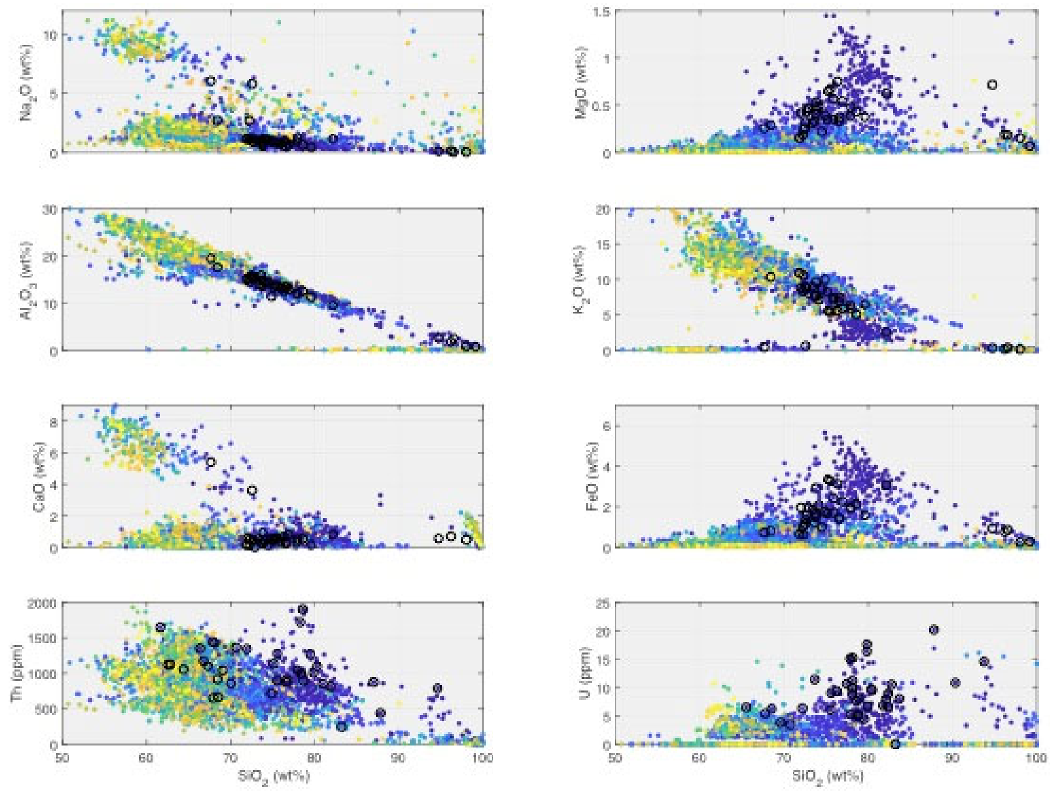

Figure DR1.5 Compositional data from sample Lyell08. Polish compositions for each laser spot analysis are defined as black circles and presented in Figure 3 of the main text. As in figure 2, yellow colors are deep reflecting the bottom of laser pits and the composition of underlying host minerals, while blue colors mark shallow depths and that of the glacial polish. Ablation rate was not calibrated for this sample, thus depths are relative.

Figure DR 1.6

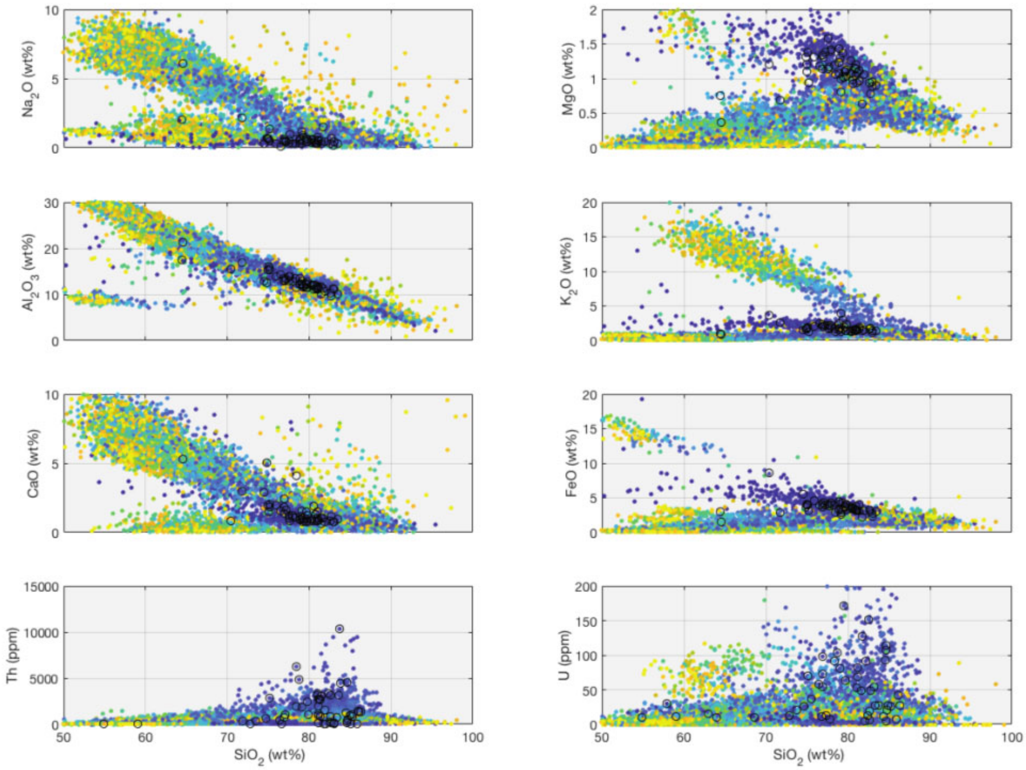

Figure DR1.6 Compositional data from sample Lyell09. Polish compositions for each laser spot analysis are defined as black circles and presented in Figure 3 of the main text. As in figure 2, yellow colors are deep reflecting the bottom of laser pits and the composition of underlying host minerals, while blue colors mark shallow depths and that of the glacial polish. Ablation rate was not calibrated for this sample, thus depths are relative.

Figure DR 1.7

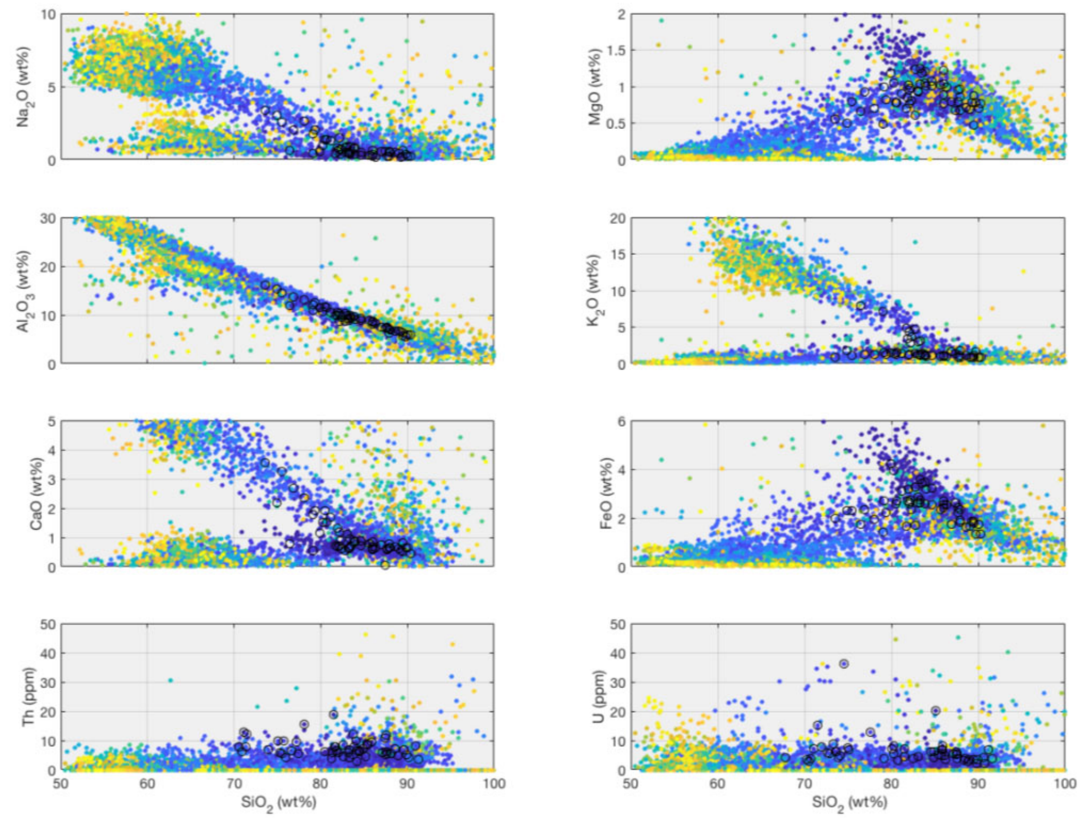

Figure DR1.7 Compositional data from sample Lyell10. Polish compositions for each laser spot analysis are defined as black circles and presented in Figure 3 of the main text. As in figure 2, yellow colors are deep reflecting the bottom of laser pits and the composition of underlying host minerals, while blue colors mark shallow depths and that of the glacial polish. Ablation rate was not calibrated for this sample, thus depths are relative.

Figure DR 2.1

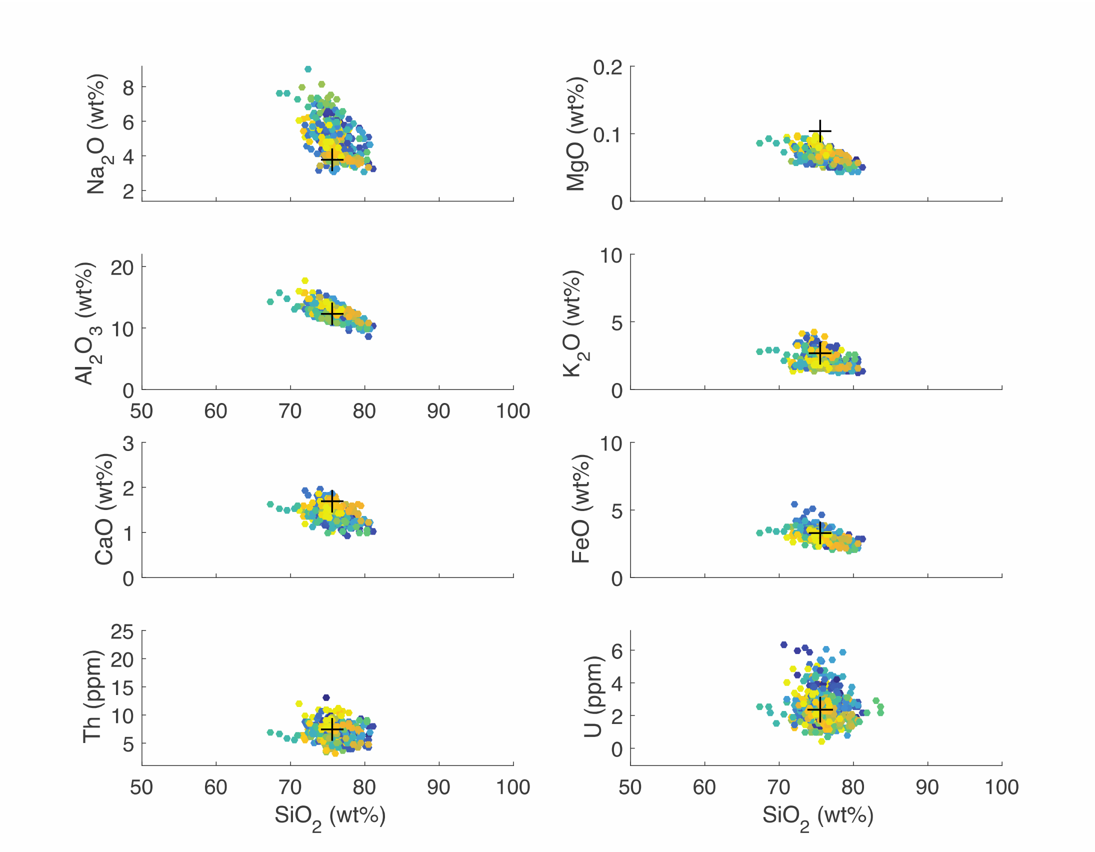

Figure DR2.1 Compositional data for secondary standard data ATHO. Crosses mark accepted values. As in figure 2, yellow colors are deep while blue colors mark shallow depths. Data are reduced using the sum normalization technique discussed in DR2. The apparent lack of depth vs. compositional bias suggests that this technique, while not delivering the most precise data do not deliver data that are inherently biased by laser ablation depth. The apparently inaccurate Mg value likely reflects the use of NIST610 Mg concentrations that are incorrect. Ablation rate was not calibrated for this sample, thus depths are relative.

Figure DR 2.2

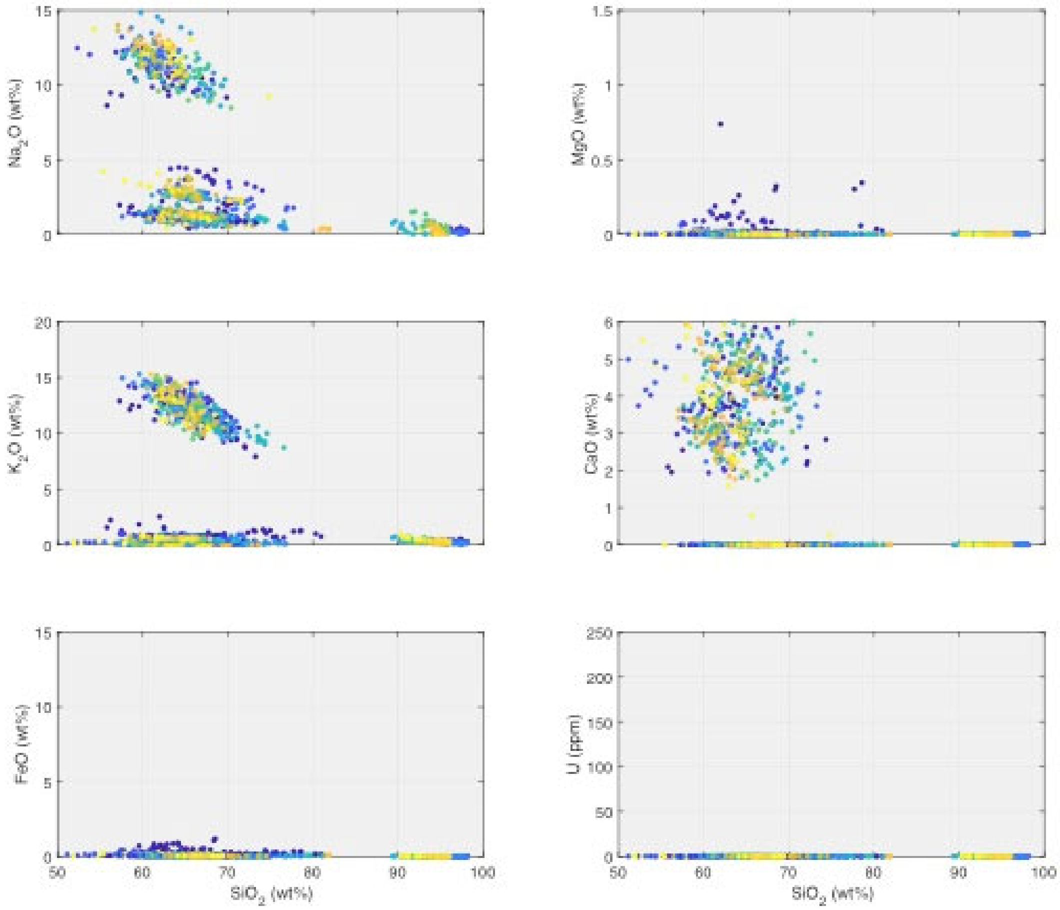

Figure DR2.1 Compositional data from a manually, non-glacially polished sample of cathedral peak shown at the same scale as figure 2 to illustrate the differences between glacially polished samples and those of the host minerals. The apparent lack of depth vs. compositional bias suggests that this technique is not inherently biased by laser ablation depth. Note that the distinct host mineral compositions are separately resolved and that shallow analyses do not artificially yield compositions consistent with the glacial polish as shown in figure 2. For example, the Mg, Fe and U enrichment in the surface of glacial polish (Fig. DR1.2-1.7) is not recorded on the manually polished sample. Ablation rate was not calibrated for this sample, thus depths are relative.

Table DR 3.1: SHRIMP-RG ^{230}Th, ^{232}Th, ^{234}U, ^{238}U data, note ^{234}U was not acquired during sessions 1-2 and thus not included in Figure 4. Spot analyses below 10 ppm U are not included in figure 4 and struck through and red in the tables below. All Daff analyses are from the same Daff01 samples described in the text and figures 1-2.

Session 1 March 6-7, 2017 Primary: O_2^-

Spot	U/Si	1s	(238U)/ (232Th) [a]	1s	(230Th)/ (238U) [a]	1s	corr(238U)/ (232Th) [b]	1s	(230Th)/ (232Th) [a]	1s	corr(230Th)/ (238U) [c]	1s	(234U)/ (238U) [a]	1s	U (ppm)	Th/U	Scans	Notes
Daff-01b-1.12-2	0.0025	0.0012	8.414	1.380	~~1.406~~	~~0.977~~	~~7.662~~	~~1.380~~	~~41.700~~	~~25.448~~	~~1.544~~	~~0.977~~			0.2	0.41	6/9	low-U, no 230Th, likely not polish
Daff-01b-1.12-4	0.0045	0.0005	5.320	0.308	~~4.942~~	~~3.658~~	~~4.845~~	~~0.308~~	~~13.040~~	~~11.575~~	~~5.427~~	~~3.658~~			0.4	0.65	6/9	low-U, no 230Th, likely not polish
Daff-01a-1.6-1	0.0186	0.0039	10.247	1.015	0.464	0.686	9.331	1.015	1.973	3.595	0.509	0.686			1.5	0.34	4/9	low-U
Daff-01a-1.12-1	0.0198	0.0020	7.604	0.217	~~1.376~~	~~0.525~~	~~6.924~~	~~0.218~~	~~10.716~~	~~3.993~~	~~1.511~~	~~0.525~~			1.6	0.45	7/9	low-U, no 230Th, likely not polish
Daff-01b-1.12-1	0.036	0.008	6.274	1.142	~~2.873~~	~~0.869~~	~~5.714~~	~~1.142~~	~~26.625~~	~~8.502~~	~~3.155~~	~~0.869~~			2.8	0.55	6/8	low-U, no 230Th, likely not polish
Daff-01b-1.8-2	0.0364	0.0036	11.706	0.986	~~0.428~~	~~0.371~~	~~10.660~~	~~0.986~~	~~6.949~~	~~5.465~~	~~0.470~~	~~0.372~~			2.9	0.29	5/9	big error in 230Th/232Th
Daff-01a-1.12-3	0.0467	0.0088	5.625	0.483	0.445	0.323	5.122	0.483	2.444	1.638	0.489	0.324			3.7	0.61	7/9	low-U
Daff-01b-1.12-3	0.0571	0.0068	15.492	1.931	0.455	0.188	14.108	1.931	4.161	1.643	0.500	0.188			4.5	0.22	7/9	low-U
Daff-01b-1.8-1	0.0807	0.0298	17.375	0.921	~~0.611~~	~~0.316~~	~~15.822~~	~~0.921~~	~~10.711~~	~~5.972~~	~~0.670~~	~~0.316~~			6.4	0.20	6/9	big error in 230Th/232Th
Daff-01a-1.5-2	0.0913	0.0331	10.235	1.008	~~0.776~~	~~0.300~~	~~9.321~~	~~1.008~~	~~8.682~~	~~3.451~~	~~0.852~~	~~0.300~~			7.2	0.34	5/9	in secular equilibrium
Daff-01a-1.12-2	0.1720	0.0560	16.518	1.558	0.188	0.088	15.042	1.558	3.758	1.488	0.206	0.089			13.6	0.21	7/9	
Daff-01a-1.7-1	0.1802	0.0816	24.814	2.997	0.209	0.162	22.597	2.997	7.573	3.404	0.229	0.163			14.2	0.14	5/9	
Daff-01a-1.8-1	0.1876	0.0347	13.208	1.185	0.402	0.068	12.028	1.185	4.747	0.803	0.442	0.070			14.8	0.26	6/9	
Daff-01a-1.7-2	0.1959	0.0320	11.035	1.868	~~0.287~~	~~0.098~~	~~10.049~~	~~1.869~~	~~11.865~~	~~2.847~~	~~0.315~~	~~0.099~~			15.5	0.31	7/9	in secular equilibrium
Daff-01b-1.8-4	0.2616	0.0316	60.702	3.538	0.228	0.073	55.278	3.538	16.079	6.003	0.251	0.075			20.7	0.06	5/9	big error in 230Th/232Th
BZVV-1.2	6.86	1.77	2247	504	0.921	0.026	2046	504	2262	762	1.011	0.031			542.1	0.0015	8/8	
BZVV-3.2	7.57	1.52	14094.4	1786.1	0.939	0.024	12834.9	1786.1	14562.9	726.8	1.031	0.029			598.2	0.0002	8/8	
BZVV-4.1	8.57	2.88	5693.6	1374.4	0.889	0.024	5184.8	1374.4	6312.5	311.7	0.977	0.029			677.2	0.0006	8/8	
BZVV-3.1	10.18	2.89	10990.9	1885.6	1.024	0.026	10008.8	1885.6	12316.7	2337.6	1.125	0.031			804.2	0.0003	8/8	
BZVV-1.1	11.78	2.64	16658.4	1745.3	0.901	0.020	15169.9	1745.3	16224.4	1492.3	0.989	0.026			930.6	0.0002	8/8	
BZVV-2.1	18.83	3.85	8522.7	1598.3	0.903	0.024	7761.1	1598.3	8934.7	1974.1	0.991	0.029			1487.7	0.0004	8/8	
									average (230Th/238U) for BZVV:		*0.911*	*0.017*						

Session 2 March 7-8, 2017 Primary: O^-

Spot	U/Si	1s	(238U)/ (232Th) [a]	1s	(230Th)/ (238U) [a]	1s	corr(238U)/ (232Th) [b]	1s	(230Th)/ (232Th) [a]	1s	corr(230Th)/ (238U) [c]	1s	(234U)/ (238U) [a]	1s	U (ppm)	Th/U	Scans	Notes
Daff_01b-2.5	0.000	0.000	1.897	0.289	~~-85.013~~	~~68.433~~	~~1.728~~	~~0.290~~	~~-166.603~~	~~161.919~~	~~-93.355~~	~~68.433~~			0.0	1.81	10/10	low-U, no 230Th, likely not polish
Daff-01A-2.3	0.002	0.000	12.203	0.995	~~-4.834~~	~~5.797~~	~~11.113~~	~~0.995~~	~~-69.993~~	~~87.120~~	~~-5.308~~	~~5.797~~			0.0	0.28	10/10	low-U, no 230Th, likely not polish
Daff_01b-2.2	0.036	0.005	15.911	0.598	~~-1.620~~	~~0.923~~	~~14.489~~	~~0.598~~	~~-6.959~~	~~18.366~~	~~-1.779~~	~~0.923~~			0.5	0.22	5/10	low-U, no 230Th, likely not polish
Daff-01A-2.4	0.044	0.017	17.906	1.703	~~0.682~~	~~0.434~~	~~16.306~~	~~1.703~~	~~11.011~~	~~6.909~~	~~0.749~~	~~0.435~~			0.6	0.19	4/10	low-U, big error in 230Th/232Th
Daff_01b-2.7	0.084	0.006	7.415	0.174	~~1.828~~	~~1.231~~	~~6.753~~	~~0.175~~	~~13.576~~	~~9.522~~	~~2.008~~	~~1.231~~			1.2	0.46	2/10	low-U, no 230Th, likely not polish
Daff_01b-2.4	0.086	0.027	13.164	0.765	~~1.060~~	~~0.475~~	~~11.988~~	~~0.765~~	~~13.094~~	~~6.272~~	~~1.164~~	~~0.475~~			1.3	0.26	8/10	low-U, Old
Daff_01b-2.8	0.091	0.027	32.667	2.322	~~0.829~~	~~0.619~~	~~29.748~~	~~2.323~~	~~33.718~~	~~25.930~~	~~0.911~~	~~0.619~~			1.3	0.11	4/10	low-U, no 230Th, likely not polish
Daff_01b-2.9	0.107	0.071	4.685	0.341	~~1.387~~	~~0.565~~	~~4.266~~	~~0.341~~	~~8.038~~	~~2.977~~	~~1.523~~	~~0.565~~			1.5	0.73	6/10	low-U, Old
Daff_01b-2.6	0.240	0.119	9.819	1.543	~~0.782~~	~~0.386~~	~~8.942~~	~~1.543~~	~~9.359~~	~~3.690~~	~~0.858~~	~~0.386~~			3.5	0.35	6/10	in secular equilibrium
Daff-01A-1.7-3	0.490	0.046	1.513	0.246	0.445	0.097	1.378	0.247	0.859	0.201	0.488	0.098			7.1	2.28	8/10	
Daff_01b-2.3	0.528	0.145	28.563	1.526	~~0.542~~	~~0.271~~	~~26.011~~	~~1.526~~	~~15.892~~	~~8.035~~	0.596	0.271			7.7	0.12	3/10	big error in 230Th/232Th
Daff-01A-2.6	0.533	0.462	37.081	2.965	0.319	0.074	33.768	2.965	13.238	3.101	0.350	0.076			7.7	0.09	6/10	
Daff_01b-2.1	0.582	0.201	19.231	1.085	0.511	0.135	17.513	1.085	10.364	2.574	0.561	0.136			8.4	0.18	6/10	
Daff-01b-1.8-5	1.11	0.62	31.408	3.648	~~0.488~~	~~0.109~~	~~28.602~~	~~3.648~~	~~19.816~~	~~4.516~~	0.535	0.111			16.1	0.11	6/10	Old?
Daff-01A-2.5	1.315	0.824	26.450	2.804	0.374	0.073	24.087	2.804	12.217	2.479	0.410	0.075			19.0	0.13	7/10	
Daff-01A-2.2	2.198	1.398	35.786	4.057	0.165	0.037	32.588	4.057	5.241	1.098	0.181	0.040			31.8	0.10	6/10	
Daff-01A-2.1-1	2.374	1.383	36.960	2.957	~~0.376~~	~~0.048~~	~~33.657~~	~~2.957~~	~~16.914~~	~~2.233~~	0.413	0.051			34.4	0.09	6/10	Old?
NIST611-1.1	4.292	0.066	3.148	0.022	-0.007	0.003			-0.024	0.009	-0.008	0.017			62.2	1.09	9/9	
BZVV-5.4	58.01	10.09	3014.2	728.2	0.902	0.014	2744.9	728.2	2855.6	818.7	0.990	0.022			840.0	0.0011	8/8	
BZVV-5.1	153.56	23.16	9503.3	1217.9	0.920	0.012	8654.1	1217.9	8999.2	1372.0	1.010	0.021			2223.4	0.0004	8/8	

Session 3 June 3-4, 2018 Primary: O_2^-

Spot	U/Si	1s	(238U)/ (232Th) [a]	1s	(230Th)/ (238U) [a]	1s	corr(238U)/ (232Th) [b]	1s	(230Th)/ (232Th) [a]	1s	corr(230Th)/ (238U) [c]	1s	(234U)/ (238U) [a]	1s	U (ppm)	Th/U	Scans	Notes
Daff-8.1	1.54	1.13	14.517	1.422	0.684	0.040	13.484	1.422	8.219	1.466	0.736	0.040	4.432	0.521	2.7	0.23	5/10	low U
Daff-13.5	~~2.59~~	~~2.01~~	~~14.665~~	~~1.220~~	~~0.892~~	~~0.243~~	~~13.622~~	~~1.220~~	~~13.928~~	~~3.302~~	~~0.961~~	~~0.243~~	4.842	1.458	4.6	0.23	8/10	low U, secular equilibrium
Daff-12.3	4.76	1.36	19.308	0.604	0.513	0.055	17.934	0.604	6.452	1.591	~~0.553~~	~~0.056~~	~~4.860~~	~~1.091~~	8.5	0.17	5/10	big error in 234U/238U
Daff-11.5	~~8.87~~	~~2.53~~	~~6.604~~	~~0.475~~	~~1.779~~	~~0.148~~	~~6.134~~	~~0.475~~	~~15.655~~	~~2.883~~	~~1.915~~	~~0.148~~	~~7.013~~	~~0.587~~	15.7	0.51	5/10	low 230Th, likely not polish

Table DR 3.1 continued:

Daff-4.1	9.52	28.63	12.822	1.099	0.678	0.175	11.910	1.099	6.482	1.852	0.730	0.175	5.859	0.762	16.9	0.26	6/10	
Daff-12.2	~~9.94~~	~~16.51~~	~~16.514~~	~~1.866~~	~~0.579~~	~~0.155~~	~~15.339~~	~~1.866~~	~~12.648~~	~~2.841~~	0.624	0.155	3.563	1.163	17.6	0.20	8/10	old?
Daff-12.4	11.253	1.026	~~5.567~~	~~0.596~~	~~0.749~~	~~0.467~~	~~5.171~~	~~0.596~~	~~5.757~~	~~1.361~~	~~0.806~~	~~0.467~~	~~7.546~~	~~0.842~~	20.0	0.61	6/10	secular equilibrium
Daff-8.3	12.71	15.77	21.063	2.812	0.599	0.201	19.564	2.812	12.660	4.747	0.645	0.201	3.789	1.272	22.6	0.16	7/10	big error in 230Th/232Th
Daff-13.2	13.85	14.72	20.158	1.310	0.684	0.237	18.724	1.310	13.266	0.826	0.736	0.237	3.058	0.329	24.6	0.17	5/10	
Daff-13.4	16.80	10.74	17.011	1.134	0.434	0.190	15.800	1.134	7.473	0.823	0.467	0.190	5.833	0.246	29.8	0.20	4/10	
Daff-13.6	19.03	15.61	13.529	1.619	0.581	0.089	12.567	1.619	7.354	0.751	0.626	0.089	6.086	0.928	33.8	0.25	6/10	
Daff-13.3	28.71	25.76	20.121	1.076	0.657	0.154	18.690	1.076	11.449	0.562	0.708	0.154	4.006	0.220	51.0	0.17	6/10	
Daff-8.2	29.99	33.38	20.181	0.556	0.423	0.037	18.746	0.556	8.969	0.894	0.456	0.037	4.626	0.334	53.2	0.17	6/10	
Daff-13.1	62.90	74.54	32.023	2.211	0.291	0.112	29.745	2.211	9.038	0.818	0.313	0.112	3.647	0.165	111.6	0.11	4/11	
BZVV-4.1	401.25	26.10	14490.2	990.8	0.928	0.014	13459.4	990.8	13332.3	808.9	0.999	0.014	1.085	0.026	712.2	0.0002	7/7	
BZVV-3.1	545.30	35.61	14466.0	1411.2	0.930	0.037	13436.9	1411.2	14976.6	915.9	1.001	0.037	1.037	0.027	967.8	0.0002	7/7	
										average (230Th/238U) for BZVV:	*0.929*	*0.001*						

Session 4 **July 21-23, 2018** **Primary: O_2^-**

Spot	U/Si	1s	(238U)/ (232Th) [a]	1s	(230Th)/ (238U) [a]	1s	corr(238U)/ (232Th) [b]	1s	(230Th)/ (232Th) [a]	1s	corr(230Th)/ (238U) [c]	1s	(234U)/ (238U) [a]	1s	U (ppm)	Th/U	Scans	Notes
DAFF-b2.6	~~0.29~~	~~0.23~~	~~4.564~~	~~0.067~~	~~0.453~~	~~0.145~~	~~3.795~~	~~0.083~~	~~2.356~~	~~0.552~~	~~0.545~~	~~0.152~~	~~5.166~~	~~1.329~~	0.5	~~0.83~~	5/10	low-U, no 230Th, likely not polish
DAFF-b2.5	~~0.29~~	~~0.13~~	~~17.504~~	~~0.327~~	~~0.826~~	~~0.302~~	~~14.557~~	~~0.331~~	~~31.901~~	~~4.753~~	~~0.994~~	~~0.306~~	~~3.427~~	~~0.253~~	0.5	0.22	7/10	low-U, no 230Th, likely not polish
DAFF-b2.4.3	0.77	0.72	18.259	0.383	0.502	0.085	15.185	0.386	9.184	1.679	0.604	0.098	4.087	0.412	1.4	0.21	7/10	low-U, no 230Th, likely not polish
DAFF-b2.4.2	0.99	1.31	16.560	0.235	0.625	0.066	13.772	0.240	9.621	0.587	0.752	0.082	3.804	0.428	1.8	0.23	8/10	low-U, no 230Th, likely not polish
DAFF-t1.5	2.60	2.36	~~20.472~~	~~0.368~~	~~-0.050~~	~~0.173~~	~~17.026~~	~~0.371~~	~~2.511~~	~~3.108~~	~~-0.060~~	~~0.179~~	~~3.080~~	~~0.457~~	4.7	0.18	5/10	low-U
DAFF-b2.5	3.82	7.69	24.910	0.503	0.377	0.030	20.716	0.506	14.119	1.551	0.454	0.057	3.625	0.312	6.9	0.15	6/10	low-U
DAFF-t1.3	7.01	2.23	25.196	0.611	0.501	0.122	20.955	0.613	13.972	2.827	0.602	0.131	2.395	0.090	12.7	0.15	5/10	
DAFF-t1.11	12.08	11.35	29.066	0.357	0.324	0.075	24.173	0.361	9.725	0.844	0.390	0.089	2.994	0.243	21.9	0.13	6/10	
DAFF-t.1.2.6	13.08	8.75	28.616	0.382	0.509	0.066	23.799	0.385	15.142	1.920	0.612	0.081	2.925	0.451	23.7	0.13	7/10	
DAFF-t1.9	21.75	2.09	27.492	0.494	0.498	0.089	22.864	0.496	11.289	3.016	0.599	0.102	2.518	0.209	39.3	0.14	7/10	
DAFF-t1.7	23.01	10.55	15.517	0.118	0.409	0.041	12.905	0.128	6.057	1.029	0.492	0.063	4.106	0.272	41.6	0.24	7/10	
DAFF-t1.10.2	26.54	8.91	21.320	0.313	0.448	0.047	17.731	0.317	3.332	1.078	0.539	0.067	3.136	0.189	48.0	0.18	7/10	
DAFF-t1.14	26.86	26.35	38.828	0.378	0.253	0.033	32.292	0.382	9.120	0.967	0.305	0.058	2.754	0.168	48.6	0.10	6/10	
DAFF-t1.12	26.93	33.55	24.250	0.262	0.400	0.029	20.168	0.266	10.035	0.611	0.481	0.056	4.059	0.257	48.7	0.16	8/10	
DAFF-t1.10	32.71	28.86	15.582	0.162	0.473	0.076	12.959	0.169	7.864	2.525	0.569	0.090	3.983	0.343	59.2	0.24	7/10	
DAFF-t.1.2.4	32.89	7.34	46.765	0.549	0.195	0.020	38.893	0.551	10.236	0.884	0.234	0.052	1.913	0.144	59.5	0.08	9/10	
DAFF-t1.10.3	33.18	21.90	30.878	0.429	0.344	0.073	25.680	0.432	8.582	0.783	0.413	0.088	3.383	0.215	60.0	0.12	4/10	
DAFF-t1.1	34.60	29.97	35.340	0.525	0.262	0.053	29.391	0.528	12.134	1.409	0.315	0.071	2.230	0.189	62.6	0.11	6/10	
DAFF-t1.2	35.59	16.88	17.157	0.198	0.320	0.046	14.269	0.204	6.076	0.512	0.384	0.067	3.543	0.339	64.4	0.22	8/10	
DAFF-t.1.2.3	41.06	28.58	26.078	0.267	0.413	0.052	21.688	0.272	7.264	0.557	0.497	0.071	3.618	0.277	74.3	0.14	6/10	
DAFF-t.1.2.2	42.09	31.78	33.269	0.437	0.263	0.042	27.669	0.440	6.525	0.738	0.316	0.064	2.748	0.450	76.1	0.11	7/10	
DAFF-t1.13	42.58	25.39	15.000	0.168	0.315	0.046	12.475	0.175	2.761	0.620	0.379	0.067	3.520	0.774	77.0	0.25	7/10	
DAFF-t.1.2.5	43.13	43.92	18.338	0.202	0.257	0.055	15.251	0.208	5.261	0.559	0.309	0.073	3.042	0.404	78.0	0.21	9/10	
BZVV-1.1,	472.28	46.48	4854.3	145.8	0.772	0.040	4037.2	145.8	4975.3	835.4	0.928	0.063	0.971	0.019	854.3	0.0008	7/9	
BZVV-1.2,	465.73	60.23	7849.0	339.1	0.739	0.026	6527.7	339.1	5992.3	976.5	0.889	0.055	0.984	0.016	842.4	0.0005	7/9	
BZVV-1.3,	584.56	36.01	32878.9	2905.5	0.773	0.026	27344.1	2905.5	26201.3	5161.9	0.930	0.055	0.996	0.017	1057.4	0.0001	8/9	
BZVV-1.4,	446.78	30.51	7300.9	214.5	0.856	0.017	6071.9	214.5	6266.3	780.9	1.029	0.051	1.024	0.015	808.1	0.0005	7/9	
BZVV-1.5,	352.61	22.16	8473.8	245.7	0.925	0.011	7047.4	245.7	9066.5	476.9	1.112	0.049	1.020	0.016	637.8	0.0004	7/10	
										average (230Th/238U) for BZVV:	*0.832*	*0.048*						

Session 5 **July 27-30, 2018** **Primary: O_2^-**

Spot	U/Si	1s	(238U)/ (232Th) [a]	1s	(230Th)/ (238U) [a]	1s	corr(238U)/ (232Th) [b]	1s	(230Th)/ (232Th) [a]	1s	corr(230Th)/ (238U) [c]	1s	(234U)/ (238U) [a]	1s	U (ppm)	Th/U	Scans	Notes
Daff-B-1.1-2	1.06	0.31	~~23.899~~	~~0.485~~	~~0.552~~	~~0.110~~	~~18.586~~	~~0.485~~	~~15.396~~	~~2.059~~	0.710	0.112	3.358	0.109	1.5	0.17	5/8	low U, thin, in SE
Daff-L-1.11	1.77	1.37	~~25.063~~	~~0.706~~	0.629	0.021	~~19.491~~	~~0.706~~	~~15.315~~	~~0.499~~	0.809	0.028	3.700	0.532	2.6	0.16	4/10	low U, thin, in SE
Daff-B-1.2-2	3.07	2.09	~~24.484~~	~~1.011~~	~~0.498~~	~~0.000~~	~~19.041~~	~~1.011~~	~~13.306~~	~~0.000~~	0.640	0.018	4.894	0.163	4.4	0.16	3/10	low U, thin, in SE
Daff-L-1.6	3.49	2.93	14.666	0.165	0.404	0.037	11.405	0.166	6.775	1.978	0.520	0.041	3.908	0.348	5.1	0.27	4/10	low U
Daff-L-1.5	5.41	2.90	19.719	0.274	0.453	0.023	15.335	0.274	10.227	0.534	0.583	0.029	4.027	0.115	7.8	0.20	4/10	
Daff-L-1.13	6.85	5.89	18.522	2.544	0.485	0.057	14.404	2.544	9.748	0.421	0.624	0.060	3.418	0.245	9.9	0.22	4/10	
Daff-T-1.5-3	15.10	3.71	22.597	0.473	0.901	0.072	17.573	0.473	7.076	1.224	1.159	0.074	3.036	0.304	21.9	0.18	5/10	
Daff-T-1.2	15.86	15.50	~~29.974~~	~~0.285~~	~~0.748~~	~~0.041~~	~~23.310~~	~~0.286~~	~~18.581~~	~~1.045~~	~~0.962~~	~~0.045~~	~~3.467~~	~~0.228~~	23.0	0.13	5/10	Old?
Daff-T-1.6-3	16.72	28.27	16.943	0.245	0.590	0.056	13.177	0.245	6.428	0.871	0.759	0.059	4.119	0.404	24.3	0.24	6/10	
Daff-B-1.2	18.59	2.18	14.401	0.152	0.437	0.031	11.199	0.153	6.129	0.412	0.562	0.036	3.931	0.362	27.0	0.28	5/8	

Table DR 3.1 continued:

Daff-T-1.6	25.71	21.89	25.264	0.249	0.438	0.082	19.647	0.250	6.488	1.384	0.564	0.084	3.967	0.245	37.3	0.16	7/10	
Daff-T-1.6-2	27.78	50.37	37.210	0.430	0.396	0.039	28.938	0.430	14.267	0.909	0.509	0.043	2.832	0.082	40.3	0.11	5/10	
Daff-T-1.1-4	38.04	85.79	22.526	0.238	0.429	0.036	17.518	0.238	9.966	1.831	0.552	0.041	3.982	0.303	55.2	0.18	6/10	
Daff-T-1.8	40.56	25.60	15.145	1.644	0.523	0.167	11.778	1.645	7.420	1.694	0.672	0.168	3.977	0.059	58.8	0.27	3/10	
Daff-T-1.1	41.77	4.07	113.476	3.222	0.224	0.082	88.249	3.222	36.275	0.996	0.288	0.084	1.624	0.048	60.6	0.04	5/10	last five scans
Daff-T-1.9	44.78	32.06	23.803	0.199	0.339	0.020	18.511	0.199	7.436	0.416	0.436	0.027	3.659	0.385	65.0	0.17	6/10	
Daff-T-1.8-3	71.54	61.81	19.597	0.282	0.371	0.099	15.241	0.282	5.944	0.729	0.477	0.101	4.689	0.223	103.8	0.21	6/10	
Daff-T-1.1	88.99	37.40	30.785	0.258	0.404	0.033	23.941	0.259	13.764	1.217	0.519	0.038	2.974	0.369	129.1	0.13	5/10	first 5 scans
Daff-T-1.8-2	90.64	41.63	18.450	0.151	0.291	0.122	14.349	0.152	5.630	0.658	0.375	0.123	3.740	0.457	131.5	0.22	6/10	
Daff-T-1.8-6	104.62	54.23	24.417	0.351	0.353	0.027	18.989	0.352	4.461	0.635	0.454	0.032	3.073	0.100	151.8	0.17	7/10	
Daff-L-1.2	128.40	30.92	32.695	0.393	0.442	0.122	25.426	0.393	8.794	1.988	0.568	0.123	2.504	0.121	186.3	0.12	6/10	
Daff-T-1.8-5	134.26	73.25	29.383	0.428	0.275	0.051	22.851	0.429	7.813	0.599	0.353	0.054	3.400	0.333	194.8	0.14	6/10	
NIST611-1.1	3.37	1.03	3.102	0.072	-0.03	20.74			-0.08	32.99	-0.036	20.743	19.98	0.52	4.9	1.0108	6/7	
BZVVs-1.1	392.1	56.1	1054.9	18.9	0.772	0.085	820.4	18.9	918.9	137.3	0.993	0.087	1.119	0.028	569.0	0.0038	5/7	
BZVV-3.1	490.76	76.19	6883.9	246.3	0.769	0.024	5353.5	246.3	5877.9	1460.2	0.988	0.030	1.063	0.011	712.1	0.0006	6/7	
BZVV-2.1	546.34	48.03	12835.8	619.6	0.769	0.005	9982.2	619.6	10321.2	1428.4	0.989	0.019	1.031	0.014	792.8	0.0003	6/7	
BZVV-1.9	611.74	88.44	7277.748	234.176	0.753	0.018	5659.8	234.2	5523.7	636.7	0.969	0.025	1.052	0.004	887.6	0.0006	6/7	
BZVVs-1.4	695.10	50.78	11229.3	596.4	0.802	0.032	8732.9	596.4	9521.6	1954.6	1.031	0.036	0.987	0.032	1008.6	0.0004	5/7	
BZVVs-1.2	737.4	81.5	78255.2	7218.8	0.777	0.011	60857.8	7218.8	59778.9	8350.4	0.999	0.021	0.874	0.042	1069.9	0.0001	6/7	
BZVV-1.10			16054.6	1492.7	0.794	0.021	12485.4	1492.7	14362.3	4276.5	1.021	0.027	0.979	0.012		0.0003	6/7	
BZVVs-1.3			7440.516	326.336	0.803	0.018	5786.4	326.3	6007.3	890.2	1.033	0.025	1.020	0.013		0.0005	6/7	
BZVV-1.8			122414.6	19004.1	0.759	0.010	95199.7	19004.1	93262.4	13476.4	0.977	0.020	0.993	0.006		0.0000	6/7	
										average (230Th/238U) for BZVV:	*0.778*	*0.018*						

ratios highlighted red and crossed-out were omitted from Fig. 4 (see Notes and text or criteria)
234U was not measured in sessions 1 and 2, and therefore the 234U/238U values are blank
parentheses denote activity ratios
[a]: measured ratios
[b]: measured (238U)/(232Th) * [session average (230Th)/(238U) for BZVV] to correct for mass discrimination
[c]: measured (230Th)/(238U) / [session average (230Th)/(238U) for BZVV] to correct for mass discrimination

Figure DR 3.1

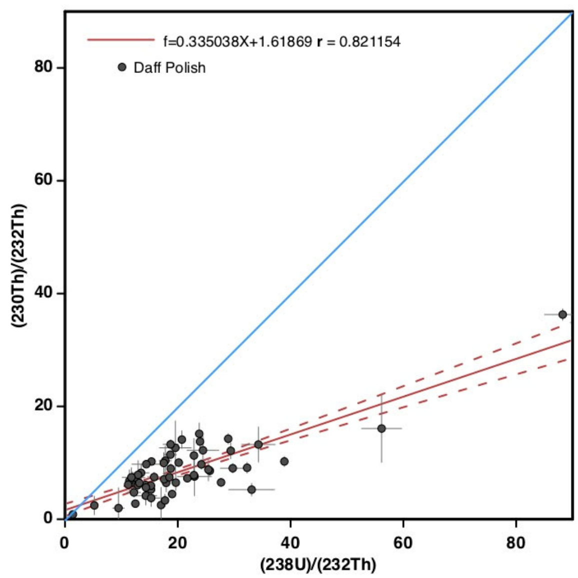

Figure DR 3.1 $^{230}Th/^{232}Th$ vs $^{238}U/^{232}U$ for Daff dome sample set (Table 3). $^{230}Th/^{232}Th$ intercept near zero justifies age determinations presented in figure 4 and that ^{230}Th as excluded from polish formation

Figure DR 4.1

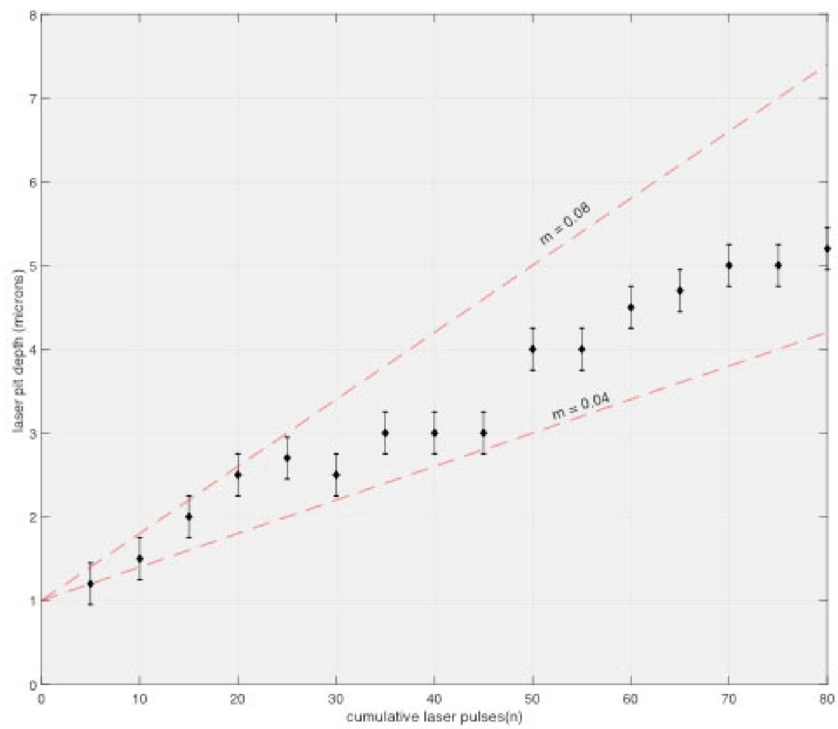

Figure DR4.1 Laser pit depth vs. number of laser bursts for a glacial polish sample from Daff dome. Measurement of the laser pit depth at 5 burst intervals provides a rough estimate of the ablation rate and is used to assign approximate depths to compositional data (Fig. 1-2). A total of 80 pulses were used for all analyses presented in this manuscript. The ablation rate varies between 0.08 μm/pulse at shallow depths decreasing to 0.05-0.06 μm/pulse at greater depths. A maximum 0.08 μm/pulse was assumed to the depth assignments in figures 1 and 2 of the main text. This rate does not influence the data reduction in any way and only permits rough estimates on the depth of chemical transitions to be assigned.